

Article

# Production of Hydrogen-Rich Gas by Formic Acid Decomposition over CuO-CeO<sub>2</sub>/γ-Al<sub>2</sub>O<sub>3</sub> Catalyst

Alexey Pechenkin <sup>1,2</sup>, Sukhe Badmaev <sup>1,2,\*</sup>, Vladimir Belyaev <sup>1</sup> and Vladimir Sobyenin <sup>1</sup>

<sup>1</sup> Borekov Institute of Catalysis, Novosibirsk 630090, Russia; pechenkin@catalysis.ru (A.P.); belyaev@catalysis.ru (V.B.); sobyanin@catalysis.ru (V.S.)

<sup>2</sup> Department of Natural Sciences, Novosibirsk State University, Novosibirsk 630090, Russia

\* Correspondence: sukhe@catalysis.ru

Received: 29 August 2019; Accepted: 12 September 2019; Published: 19 September 2019



**Abstract:** Formic acid decomposition to H<sub>2</sub>-rich gas was investigated over a CuO-CeO<sub>2</sub>/γ-Al<sub>2</sub>O<sub>3</sub> catalyst. The catalyst was characterized by XRD, HR TEM and EDX methods. A 100% conversion of formic acid was observed over the copper-ceria catalyst under ambient pressure, at 200–300 °C, N<sub>2</sub>:HCOOH = 75:25 vol.% and flow rate 3500–35,000 h<sup>-1</sup> with H<sub>2</sub> yield of 98%, wherein outlet CO concentration is below the equilibrium data (<0.5 vol.%). The copper-ceria catalyst proved to be promising for multifuel processor application, and the H<sub>2</sub> generation from dimethoxymethane, methanol, dimethyl ether and formic acid on the same catalyst for fuel cell supply.

**Keywords:** formic acid decomposition; hydrogen production; CuO-CeO<sub>2</sub>/γ-Al<sub>2</sub>O<sub>3</sub>; multifuel processor; copper catalyst; oxygenates; fuel cell

## 1. Introduction

Growing interest in, and demand for, high temperature proton exchange membrane fuel cells (HT PEM FC) has evidently manifested itself during the past decade due to their high tolerance to fuel impurities compared to the low temperature (LT) PEM FC [1–3]. For instance, the HT PEM FC can be fueled by hydrogen-rich gas containing up to 3 vol.% of CO [1]. Analysis of current literature shows that gas mixture with this composition can be produced by catalytic conversion of oxygenates such as methanol [4–6], dimethyl ether (DME) [7–9], dimethoxymethane (DMM) [10–14] and formic acid (FA) [15–23]. The obtained H<sub>2</sub>-rich gas can be directly used as fuel without complex CO removal processes. This makes the HT PEM FC-based power units more compact and simple. The typical HT PEM FC-based power unit scheme is shown in Figure 1.

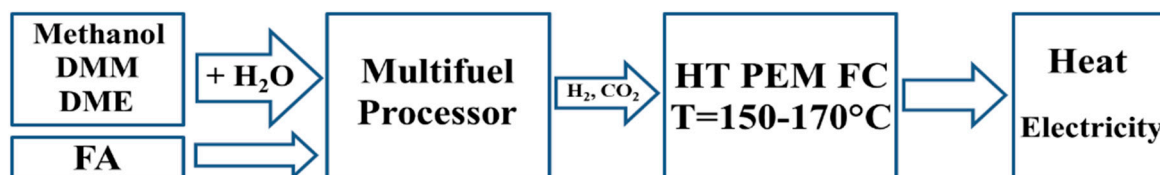


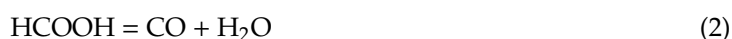
**Figure 1.** Scheme of power unit based on high temperature proton exchange membrane fuel cells fueled by oxygenates.

In our previous work [12,13], effective bifunctional CuO-CeO<sub>2</sub>/γ-Al<sub>2</sub>O<sub>3</sub> catalysts have been proposed for methanol, dimethyl ether and dimethoxymethane steam reforming (SR) to H<sub>2</sub>-rich gas showing great promise for a multifuel processor approach. The catalysts comprised of acidic and Cu-based sites and provided complete methanol/DME/DMM conversion and a H<sub>2</sub> production rate of 15 L/(g<sub>cat</sub>·h) at 300–370 °C.

Supported Cu-based catalysts proved highly active and selective for formic acid (FA) decomposition (Reaction (1)) [20]. In particular, the reaction in this work was studied over carbon-supported copper catalysts doped with nitrogen atoms (Cu/N-PCN). The catalysts provided complete conversion of FA at temperatures  $>270$  °C and high hydrogen productivity (up to 97.4%).



Reaction (1) can be accompanied by side Reactions (2) and (3) yielding CO and water:



The present work reports the performance of the CuO-CeO<sub>2</sub>/γ-Al<sub>2</sub>O<sub>3</sub> catalysts in FA decomposition to H<sub>2</sub>-rich gas to be used for HT PEM FC. The effect of some reaction conditions on the catalyst's performance was studied. The catalyst was characterized by XRD, HRTEM and EDX techniques. In order to evaluate the catalyst's possibility for multifuel processor applications, we compared CuO-CeO<sub>2</sub>/γ-Al<sub>2</sub>O<sub>3</sub> catalytic properties in methanol, dimethyl ether and dimethoxymethane steam reforming and FA decomposition reactions.

## 2. Materials and Methods

The catalyst of composition 10 wt.% CuO-5 wt.% CeO<sub>2</sub>/γ-Al<sub>2</sub>O<sub>3</sub>, which showed the best performance in methanol, DME and DMM SR reactions in our earlier study [13], was used in the FA decomposition experiments. It was prepared by the impregnation method reported in details elsewhere [13]. Samples for transmission electron microscopy (TEM) were prepared by carefully applying the catalyst powder on a carbon film on a nickel grid. These samples were investigated by conventional and high-resolution (HR) TEM and energy-dispersive X-ray (EDX) chemical microanalysis, using an electron microscope JEM 2010 (JEOL Ltd., Tokyo, Japan) at operation voltage 200 kV and lattice-fringe resolution 0.14 nm. The microscope was equipped with an EDX unit (EDAX Co, Mahwah, NJ, USA) for the local elemental analysis (the energy resolution was 130 eV).

X-ray diffraction (XRD) data were collected using a URD-63 diffractometer with a CuK<sub>α</sub> source (graphite monochromator). The measurements were taken within 2θ scanning area = 20°–80° with a step of 0.02° (2θ) and an accumulation time of 1.0 s. The diffraction patterns were processed using the PowderCell 2.4 software package. The identification of the crystalline phases was performed using the JCPDS international diffraction database.

Experiments on FA decomposition were carried out in a flow U-shaped reactor (inner diameter 4 mm) at 120–320 °C under ambient pressure. The temperature of the catalytic bed was measured using a chromel/alumel thermocouple placed in the middle of this bed. Before reaction, the copper-ceria catalyst was pre-reduced in situ at 300 °C in a mixture of hydrogen (5 vol.%) diluted with N<sub>2</sub> at a total flow rate of 3000 mL/h during 1 h. After that, the reactor was cooled to 120–200 °C in a flowing mixture of hydrogen and nitrogen and then the gas mixture was switched to (vol.%): 25 HCOOH and 75 N<sub>2</sub>. The total gas hourly space velocity (GHSV) was 3500–35,000 h<sup>-1</sup>.

FA was fed into the reactor by passing N<sub>2</sub> (99.999%) through a glass saturator filled with formic acid (JSC Reahim, 99%) maintained at 60 °C. N<sub>2</sub> and H<sub>2</sub> were introduced to the reactor by gas flow-mass meters (Bronkhorst). The inlet and outlet concentrations of H<sub>2</sub>, CO, CO<sub>2</sub> and H<sub>2</sub>O were recorded using gas chromatography (Chromos-1000, Chromos Engineering, Dzerzhinsk, Russia) equipped with thermal conductivity and flame ionization detectors (Porapak T and CaA molecular sieves columns). The minimum concentration of CO, CO<sub>2</sub>, H<sub>2</sub> and H<sub>2</sub>O that could be determined using this method was 5·10<sup>-3</sup> vol.%. During the experiments, the carbon balance was controlled with an accuracy of ±3%.

Conversion of HCOOH, H<sub>2</sub> selectivity, hydrogen yield and productivity were calculated by the following formulas:

$$X_{\text{HCOOH}}(\%) = \frac{C_{\text{HCOOH}}^{\text{in}} - C_{\text{HCOOH}}^{\text{out}} \times \frac{C_{\text{N}_2}^{\text{in}}}{C_{\text{N}_2}^{\text{out}}}}{C_{\text{HCOOH}}^{\text{in}}} \times 100 \quad (4)$$

$$S_{\text{H}_2}(\%) = \frac{C_{\text{CO}_2}^{\text{out}}}{C_{\text{CO}_2}^{\text{out}} + C_{\text{CO}}^{\text{out}}} \times 100 \quad (5)$$

$$Y_{\text{H}_2}(\%) = \frac{S_{\text{H}_2} \times X_{\text{HCOOH}}}{100} \quad (6)$$

$$W_{\text{H}_2} \left( \frac{\text{L}}{\text{h} \cdot \text{g}_{\text{cat}}} \right) = \frac{F \times C_{\text{H}_2}^{\text{out}} \times \frac{C_{\text{N}_2}^{\text{in}}}{C_{\text{N}_2}^{\text{out}}}}{100 \times m_{\text{cat}}} \quad (7)$$

where  $C^{\text{in}}$ ,  $C^{\text{out}}$  are the concentrations before and after reactor, respectively;  $F$  is the flow rate of the reaction mixture (L/h);  $m_{\text{cat}}$  is the catalyst weight (g).

### 3. Results

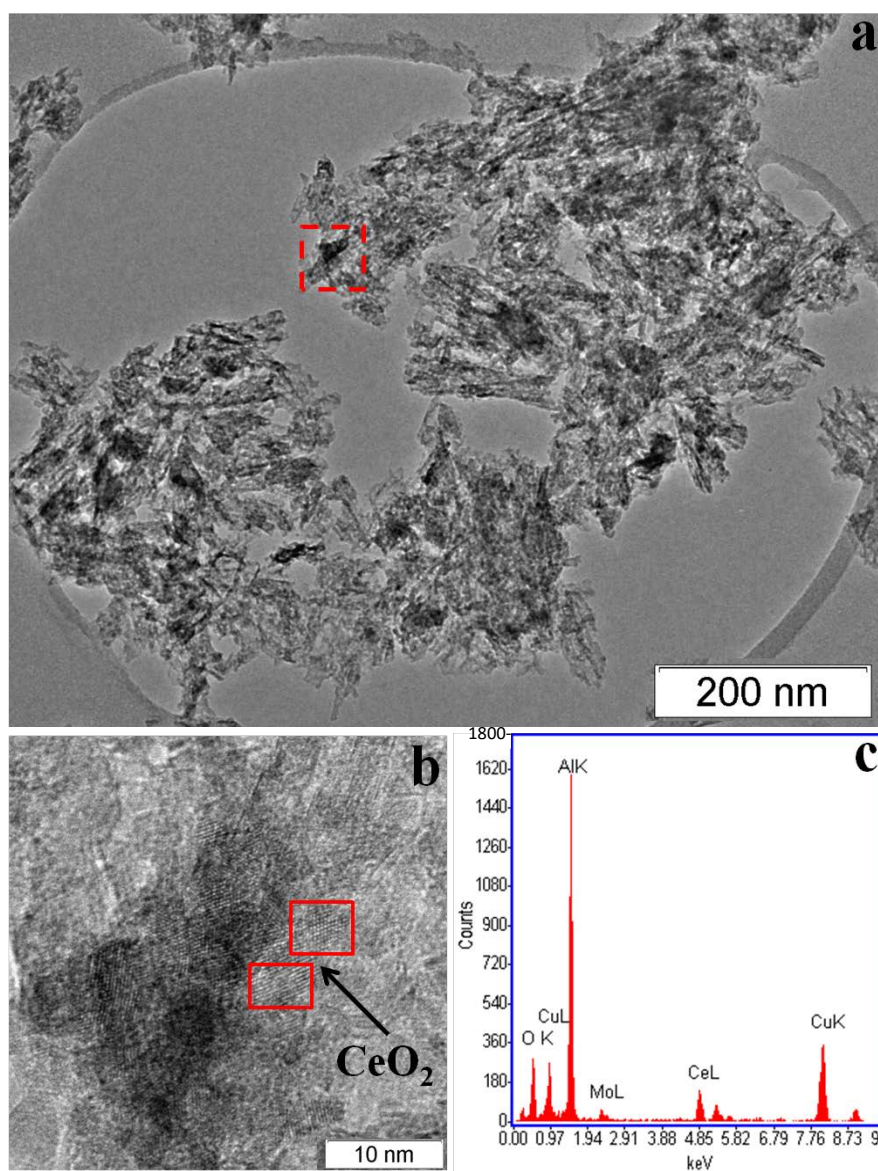
#### 3.1. Catalyst Characterization

Table 1 presents the data obtained from XRD patterns of fresh and used CuO-CeO<sub>2</sub>/γ-Al<sub>2</sub>O<sub>3</sub> catalysts. It shows that the fresh catalyst contains phases of cerium dioxide and γ-Al<sub>2</sub>O<sub>3</sub>. A strong decrease in the value of cerium dioxide unit cell parameter to 5.390 Å, as compared to the standard value of 5.411 Å, was observed. This may be due to the insertion of copper ions with a smaller ionic radius and a lesser degree of oxidation in the structure of cerium dioxide ( $r(\text{Cu}^{2+}) = 0.76 \text{ \AA}$ ,  $r(\text{Ce}^{4+}) = 1.01 \text{ \AA}$ ). CeO<sub>2</sub> is in a highly dispersed state; its CSR size is 40 Å. The phases of crystallized copper species were not detected. Apparently, this fact indicates that copper oxide is in a form of either well dispersed or amorphous species on γ-Al<sub>2</sub>O<sub>3</sub> surface. For the used catalyst, we can see a slight decrease in the CeO<sub>2</sub> lattice parameter to a value of 5.395 Å. This fact most likely indicates the possible formation of a mixed oxide of copper and cerium [24–26]. The phase of highly dispersed metallic copper is also observed in the used catalyst. Most likely, this is due to the fact that part of the copper ions leave the structure of cerium oxide during the reaction.

**Table 1.** XRD data for the CuO-CeO<sub>2</sub>/γ-Al<sub>2</sub>O<sub>3</sub> catalysts.

Catalyst	Phase Composition	Unit Cell Parameters, Å	CSR (Å)
Fresh	γ-Al <sub>2</sub> O <sub>3</sub>	7.918	50
	CeO <sub>2</sub>	5.390	40
Used	γ-Al <sub>2</sub> O <sub>3</sub>	7.918	50
	CeO <sub>2</sub>	5.395	30
	Cu	n.d.	highly dispersed

Figure 2 shows the TEM image of the fresh CuO-CeO<sub>2</sub>/γ-Al<sub>2</sub>O<sub>3</sub> catalyst and the HR TEM image and EDX spectrum of the marked area. In the TEM image, we observed an agglomerate of about 50 nm in size (the marked area). The HR TEM image and EDX spectrum of this area were recorded. The EDX spectrum shows that this agglomerate consists of Cu and Ce and an atomic ratio Cu:Ce = 70:30 at.%. In the high resolution TEM picture of the agglomerate, cerium dioxide particle (interplanar distances  $d(111) = 0.312$  and  $d(200) = 0.271$  nm, not shown in figure) was observed. We were unable to detect copper particles in the HR TEM image because of their low contrast. According to XRD data, copper oxide phases were not observed in the fresh catalyst, so it can be concluded that copper oxide particles were in a highly dispersed state.



**Figure 2.** TEM image (a) of the fresh CuO-CeO<sub>2</sub>/γ-Al<sub>2</sub>O<sub>3</sub> catalyst and the HR TEM (b) and EDX spectra (c) of the marked area.

Figure 3 shows the TEM, HR TEM images and EDX spectrum of the CuO-CeO<sub>2</sub>/γ-Al<sub>2</sub>O<sub>3</sub> catalyst after reaction. It shows that, similar to the fresh catalyst, the used catalyst contains copper-ceria agglomerates of about 30–50 nm in size and an atomic ratio Cu:Ce = 60:40 at.%. In the HR TEM image, we observed CeO<sub>2</sub> particles and no copper particles, as in the case of the fresh catalyst. However, according to XRD data, the used catalyst contains the phase of highly dispersed metallic copper. We believe that this phase refers to particles outside the agglomerates. These particles obviously suffer sintering during long-term operation of the catalyst and therefore lose activity. At the same time, the active sites of the catalyst are particles of copper stabilized by cerium oxide which do not undergo changes during the formic acid decomposition reaction.

So, the CuO-CeO<sub>2</sub>/γ-Al<sub>2</sub>O<sub>3</sub> catalyst surface contains the agglomerates of 30–50 nm in size which consist of mixed copper-cerium oxide (solid solution) particles of 5–7 nm in size, and some fine dispersed copper. We suggest that these agglomerated mixed copper-cerium oxide particles are the active copper sites of the catalyst, which is in agreement with our previous work [13].

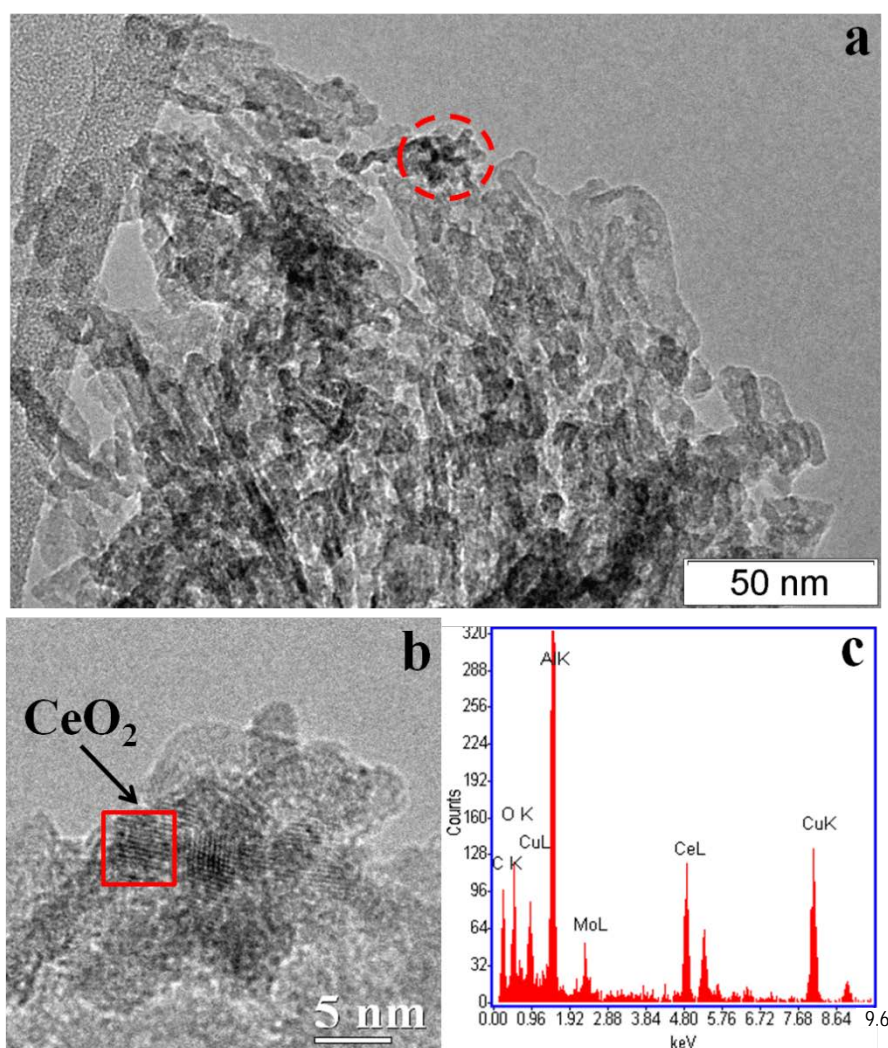


**Figure 3.** TEM image (a) of the used CuO-CeO<sub>2</sub>/γ-Al<sub>2</sub>O<sub>3</sub> catalyst and the HR TEM (b) and EDX spectra (c) of the marked area.

### 3.2. Catalytic Performance of CuO-CeO<sub>2</sub>/γ-Al<sub>2</sub>O<sub>3</sub> in FA Decomposition

Figure 4 demonstrates dependencies of FA conversion and outlet H<sub>2</sub>, CO<sub>2</sub>, CO concentrations at FA decomposition over 10%Cu-5%CeO<sub>2</sub>/γ-Al<sub>2</sub>O<sub>3</sub> catalyst at GHSV of 3500 h<sup>-1</sup> (Figure 4a) and 35,000 h<sup>-1</sup> (Figure 4b) on temperature. Equilibrium values are shown by dashed lines. The equilibrium compositions were calculated assuming equilibrium mixtures contained only H<sub>2</sub>, H<sub>2</sub>O, CO<sub>2</sub> and CO. The equilibrium and experimental values of H<sub>2</sub>O are not shown because they coincide with respective values of CO, as well as the equilibrium values of CO<sub>2</sub> which are nearly similar to those of H<sub>2</sub>.

The products of formic acid decomposition were H<sub>2</sub>, H<sub>2</sub>O, CO<sub>2</sub> and CO; no other products were observed. As shown in Figure 4, FA conversion rises with increasing temperature and gets 100% at 200 °C, GHSV = 3500 h<sup>-1</sup>, and at 300 °C, GHSV = 35,000 h<sup>-1</sup>. The product concentrations also increase with increasing temperature. In the case of GHSV = 3500 h<sup>-1</sup>, at temperatures above 200 °C, the H<sub>2</sub> and CO<sub>2</sub> concentrations are above their equilibrium composition, whereas the CO concentration is below the equilibrium value. This is because the RWGS Reaction (3) does not reach equilibrium during the experiment. Such behavior is typical for this catalyst; similar results were obtained in the steam reforming of methanol, DME and DMM [13]. As GHSV increased to 35,000 h<sup>-1</sup>, the temperature dependencies of FA conversion and product concentrations shifted to a higher temperature region.

Complete FA conversion was reached at 300 °C, whereas the CO concentration remained constant and stayed below 0.5 vol.%.

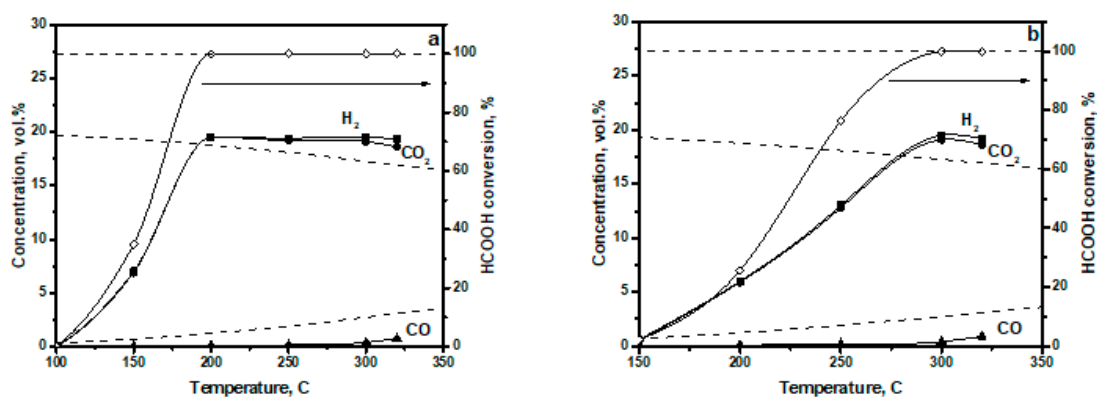


**Figure 4.** Effect of temperature on formic acid conversion and H<sub>2</sub>, CO and CO<sub>2</sub> outlet concentrations in formic acid decomposition over CuO-CeO<sub>2</sub>/γ-Al<sub>2</sub>O<sub>3</sub> catalyst at gas hour space velocity = 3500 h<sup>-1</sup> (a) and gas hour space velocity = 35,000 h<sup>-1</sup> (b). Reaction conditions:  $p = 1$  atm, inlet composition, vol.%: N<sub>2</sub>:HCOOH = 75:25. Solid lines—experiment, dotted lines—thermodynamic equilibrium values.

Figure 5 illustrates how the hydrogen yield and CO concentration depended on the reaction mixture feed rate at FA decomposition over CuO-CeO<sub>2</sub>/γ-Al<sub>2</sub>O<sub>3</sub> at 300 °C. It shows that, even with ten-fold increase in GHSV, the hydrogen yield and CO concentration remained almost unchanged and amount to 98% and 0.4 vol.%, respectively.

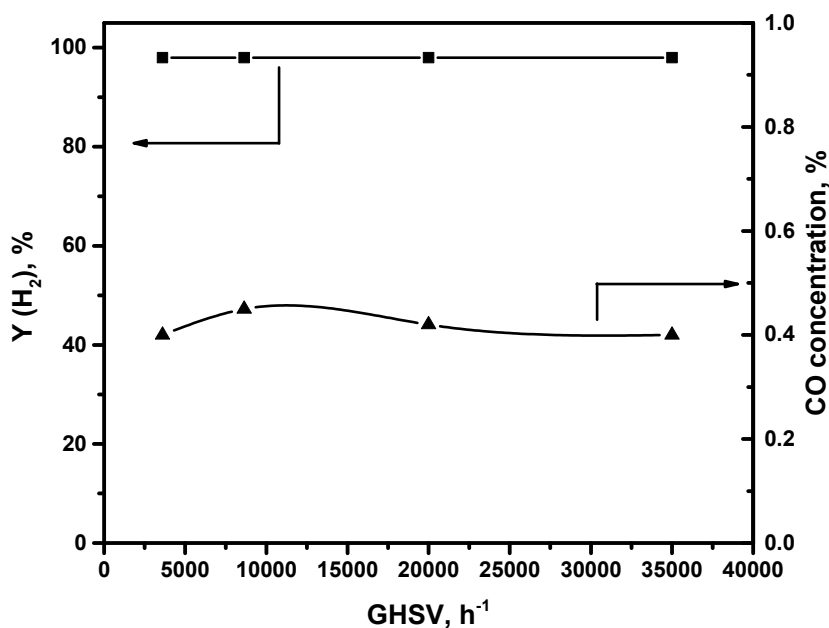


**Figure 5.** Effect of GHSV on H<sub>2</sub> yield (■) and outlet CO concentration (▲) over CuO-CeO<sub>2</sub>/γ-Al<sub>2</sub>O<sub>3</sub> catalyst for HCOOH decomposition. Reaction conditions:  $p = 1$  atm,  $T = 300$  °C,  $X(\text{HCOOH}) = 100\%$ . Inlet composition, vol.%: N<sub>2</sub>:HCOOH = 75:25.

Figure 6 illustrates the effect of time on stream on the FA conversion and the outlet concentrations of H<sub>2</sub> and CO in FA decomposition over CuO-CeO<sub>2</sub>/γ-Al<sub>2</sub>O<sub>3</sub>. The experiment was carried out at 250 °C and GHSV = 35,000 h<sup>-1</sup>. It showed that during 8 h on stream, the catalyst was stable and supported constant values of FA conversion and H<sub>2</sub> and CO concentrations. We tend to explain this catalyst

stability by the fact that the copper particles on the  $\text{CuO-CeO}_2/\gamma\text{-Al}_2\text{O}_3$  surface were stabilized by ceria and thus protected against sintering.

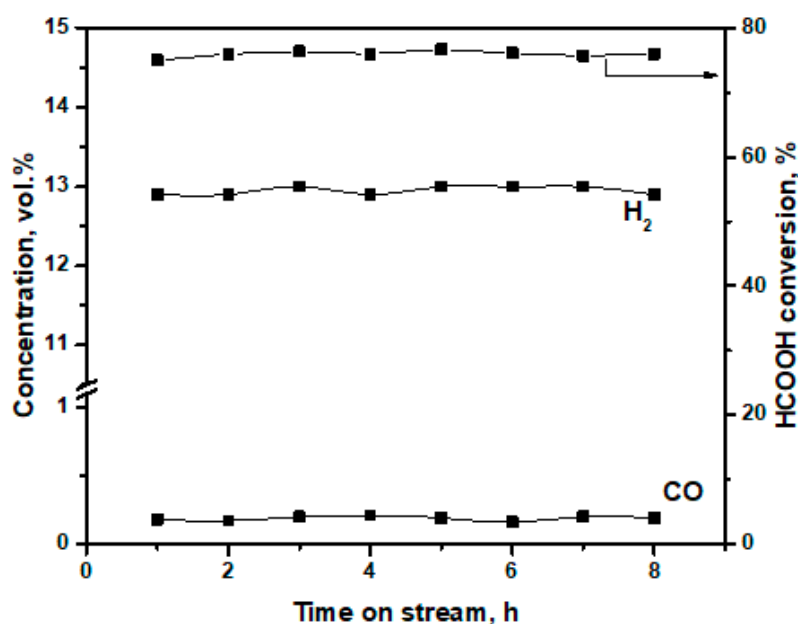


**Figure 6.** Effect of time on stream on CO and hydrogen outlet concentrations in FA decomposition over  $\text{CuO-CeO}_2/\gamma\text{-Al}_2\text{O}_3$  catalyst. Reaction conditions:  $p = 1$  atm,  $T = 250$  °C,  $\text{GHSV} = 35,000$   $\text{h}^{-1}$ ; Inlet composition, vol.%:  $\text{N}_2:\text{HCOOH} = 75:25$ .

So, the results obtained (Figures 4–6) show that complete conversion of FA over 10%  $\text{CuO-5\% CeO}_2/\gamma\text{-Al}_2\text{O}_3$  was reached at temperatures 200–300 °C, yielding  $\text{H}_2$  and  $\text{CO}_2$  as the main products. The  $\text{CO}$  concentration was below 0.5 vol.%. The catalyst provided high hydrogen yield (~100%) in a wide range of  $\text{GHSV} = 3500\text{--}35,000$   $\text{h}^{-1}$  at temperatures 200–300 °C.

In this work, the catalyst properties were studied using reaction mixture diluted with nitrogen. Note again that nitrogen was used as an internal standard to provide correct determination of the reaction parameters. Clearly, hydrogen-rich gas mixture for FC feeding should be free of nitrogen dilution. Our calculations for nitrogen-free reaction mixture showed that FA decomposition over 10%  $\text{CuO-5\% CeO}_2/\gamma\text{-Al}_2\text{O}_3$  produces hydrogen-rich gas of composition (vol.%): 48  $\text{H}_2$ , 48  $\text{CO}_2$ , 2  $\text{CO}$ , 2  $\text{H}_2\text{O}$  that is appropriate for direct feeding HT PEM FC.

Table 2 compares the results on vapor phase FA decomposition over  $\text{CuO-CeO}_2/\gamma\text{-Al}_2\text{O}_3$  and other efficient catalysts:  $\text{Cu/N-doped carbon}$  [20]; 1%  $\text{Au/SiO}_2$  [21]; and Ir-, Pt-, Rh-, Pd-/C [22]. All data refer to complete FA conversion. Note that  $\text{H}_2$  and  $\text{CO}_2$  were the main products of FA decomposition over these catalysts. According to the cited data, the product distribution insignificantly depended on the reaction conditions, and the maximum yield of  $\text{H}_2$  (92–99.5 %) was observed at 200–300 °C for all catalysts.

**Table 2.** Comparison of catalyst activities in formic acid decomposition.

Catalysts	T, °C	Reaction Condition		Y (H <sub>2</sub> ), %	Refs
		HCOOH: Inert vol.%.vol.%	FA Flow Rate, h <sup>-1</sup>		
10% CuO-5% CeO <sub>2</sub> /γ-Al <sub>2</sub> O <sub>3</sub>	200	25:75	875	98	This work
	300	25:75	8750	98	
Cu/C	270	5:95	3150 <sup>1</sup>	97.4	[20]
1% Au/SiO <sub>2</sub>	250	7:93	560	99.5	[21]
2% Ir/C	200	5:95	400	99.5	[22]
2% Pt/C				98.6	
2% Rh/C				97	
2% Pd/C				91.7	

<sup>1</sup>—data calculated per gram catalyst 3150 mL/(h g<sub>cat</sub>).

Thus, the literature data [20] and results of the present work prove that Cu-based catalysts are effective in the reaction of FA decomposition and keep up with catalysts containing the VIII group metals.

As mentioned above (see Introduction), the CuO-CeO<sub>2</sub>/γ-Al<sub>2</sub>O<sub>3</sub> catalyst was effective in dimethoxymethane, dimethyl ether, methanol SR reactions [12,13]. It seems reasonable to compare the catalytic properties of CuO-CeO<sub>2</sub>/γ-Al<sub>2</sub>O<sub>3</sub> catalyst in dimethoxymethane, dimethyl ether, methanol SR and FA decomposition reactions in order to extend the scope of multifuel processor applications.

Table 3 presents the following data: temperature of 100% conversion of dimethoxymethane, dimethyl ether, methanol and FA to H<sub>2</sub>-rich gas; H<sub>2</sub> yield; outlet CO concentration in the produced H<sub>2</sub>-rich gas; and H<sub>2</sub> productivity. Complete dimethoxymethane, dimethyl ether, methanol and FA conversion was attained at 300–370 °C. Regardless of the raw material, the catalyst yielded H<sub>2</sub>-rich gas containing low outlet CO concentration (≤1 vol.%), which can be used directly for HT PEM FC feeding [1–3]. H<sub>2</sub> productivity of the CuO-CeO<sub>2</sub>/γ-Al<sub>2</sub>O<sub>3</sub> catalyst (Table 3) in FA decomposition (~15 L H<sub>2</sub>/g<sub>cat</sub>·h) was the same as in DMM, DME, methanol SR reactions. Taking into account these H<sub>2</sub> productivity data, we calculated that just ~50 g of the CuO-CeO<sub>2</sub>/γ-Al<sub>2</sub>O<sub>3</sub> catalytic system is enough to operate a 1 kW HT PEM FC-based power unit using any substrate—DMM + H<sub>2</sub>O, DME + H<sub>2</sub>O, methanol + H<sub>2</sub>O or FA.

**Table 3.** Performance of the CuO-CeO<sub>2</sub>/γ-Al<sub>2</sub>O<sub>3</sub> catalyst in dimethoxymethane, dimethyl ether, methanol steam reforming and FA decomposition.

Reactions	Inlet Composition	T °C	GHSV h <sup>-1</sup>	Y (H <sub>2</sub> ) %	CO vol.%	W (H <sub>2</sub> ) l/(h g <sub>cat</sub> )	Refs
	vol.%						
DMM SR	C <sub>3</sub> H <sub>8</sub> O <sub>2</sub> :H <sub>2</sub> O:N <sub>2</sub> = 14:70:16	300	10,000	95	0.5	15.5	[12]
DME SR	C <sub>2</sub> H <sub>6</sub> O:H <sub>2</sub> O:N <sub>2</sub> = 20:60:20	370		90	1	15	
Methanol SR	CH <sub>3</sub> OH:H <sub>2</sub> O:N <sub>2</sub> = 40:40:20	300		95	1	15	
FA decomposition	HCOOH:N <sub>2</sub> = 25:75	300	35,000	98	0.45	15	This work

#### 4. Conclusions

A CuO-CeO<sub>2</sub>/γ-Al<sub>2</sub>O<sub>3</sub> catalyst for vapor-phase formic acid decomposition to H<sub>2</sub>-rich gas is suggested. The catalyst containing CuO-CeO<sub>2</sub> mixed oxides on the γ-Al<sub>2</sub>O<sub>3</sub> surface is active and selective in formic acid decomposition to H<sub>2</sub>-rich gas with low CO concentration (<0.5 vol.%). In particular, the CuO-CeO<sub>2</sub>/γ-Al<sub>2</sub>O<sub>3</sub> catalyst provides 100% conversion of formic acid with H<sub>2</sub> yield ~98% at 200–300 °C and GHSV = 3500–350,000 h<sup>-1</sup>. Moreover, the CuO-CeO<sub>2</sub>/γ-Al<sub>2</sub>O<sub>3</sub> catalyst shows high prospects for the multifuel processor concept. It enables the H<sub>2</sub> generation from oxygenated compounds of C1 chemistry (dimethyl ether, methanol, dimethoxymethane and formic acid) under similar reaction conditions.

**Author Contributions:** S.B. suggested the main idea of the article; A.P. carried out experiments, exported the results and prepared an initial version; V.B. suggested the methodology of the article; V.S. is in charge of supervision, writing—review and editing of the article. All authors discussed the results and revised and corrected this article.

**Funding:** This work was supported by the Ministry of Science and Higher Education of the Russian Federation (project № AAAA-A17-117041710088-0).

**Conflicts of Interest:** The authors declare no conflict of interest.

## References

1. Chandan, A.; Hattenberger, M.; El-kharouf, A.; Du, S.; Dhir, A.; Self, V.; Pollet, B.G.; Ingram, A.; Bujalski, W. High temperature (HT) polymer electrolyte membrane fuel cells (PEMFC)—A review. *J. Power Sources* **2013**, *231*, 264–278. [[CrossRef](#)]
2. Quartarone, E.; Mustarelli, P. Polymer fuel cells based on polybenzimidazole/H<sub>3</sub>PO<sub>4</sub>. *Energy Environ. Sci.* **2012**, *5*, 6436–6444. [[CrossRef](#)]
3. Rosli, R.E.; Sulong, A.B.; Daud, W.R.W.; Zulkifley, M.A.; Husaini, T.; Rosli, M.I.; Majlan, E.H.; Haque, M.A. A review of high-temperature proton exchange membrane fuel cell (HT-PEMFC) system. *Int. J. Hydrogen Energy* **2017**, *42*, 9293–9314. [[CrossRef](#)]
4. Li, D.; Li, X.; Gong, J. Catalytic Reforming of Oxygenates: State of the Art and Future Prospects. *Chem. Rev.* **2016**, *116*, 11529–11653. [[CrossRef](#)] [[PubMed](#)]
5. Palo, D.R.; Dagle, R.A.; Holladay, J.D. Methanol Steam Reforming for Hydrogen Production. *Chem. Rev.* **2007**, *107*, 3992–4021. [[CrossRef](#)]
6. Sá, S.; Silva, H.; Brandão, L.; Sousa, J.M.; Mendes, A. Catalysts for methanol steam reforming—A review. *Appl. Catal. B.* **2010**, *99*, 43–57. [[CrossRef](#)]
7. Galvita, V.; Semin, G.; Belyaev, V.; Yurieva, T.; Sobyenin, V. Production of hydrogen from dimethyl ether. *Appl. Catal. A.* **2001**, *216*, 85–90. [[CrossRef](#)]
8. Semelsberger, T.A.; Ott, K.C.; Borup, R.L.; Greene, H.L. Generating hydrogen-rich fuel-cell feeds from dimethyl ether (DME) using Cu/Zn supported on various solid-acid substrates. *Appl. Catal. A.* **2006**, *309*, 210–223. [[CrossRef](#)]
9. Volkova, G.; Badmaev, S.; Belyaev, V.; Plyasova, L.; Budneva, A.; Paukshtis, E.; Zaikovskiy, V.; Sobyenin, V. Bifunctional catalysts for hydrogen production from dimethyl ether. *Stud. Surf. Sci. Catal.* **2007**, *167*, 445–450.
10. Sun, Q.; Auroux, A.; Shen, J. Surface acidity of niobium phosphate and steam reforming of dimethoxymethane over CuZnO/Al<sub>2</sub>O<sub>3</sub>-NbP complex catalysts. *J. Catal.* **2006**, *244*, 1–9. [[CrossRef](#)]
11. Fu, Y.; Shen, J. Production of hydrogen by catalytic reforming of dimethoxymethane over bifunctional catalysts. *J. Catal.* **2007**, *248*, 101–110. [[CrossRef](#)]
12. Badmaev, S.D.; Pechenkin, A.A.; Belyaev, V.D.; Ven'yaminov, S.A.; Snytnikov, P.V.; Sobyenin, V.A.; Parmon, V.N. Steam reforming of dimethoxymethane to hydrogen-rich gas for fuel cell feeding application. *Dokl. Phys. Chem.* **2013**, *452*, 251–253. [[CrossRef](#)]
13. Pechenkin, A.A.; Badmaev, S.D.; Belyaev, V.D.; Sobyenin, V.A. Performance of bifunctional CuO-CeO<sub>2</sub>/γ-Al<sub>2</sub>O<sub>3</sub> catalyst in dimethoxymethane steam reforming to hydrogen-rich gas for fuel cell feeding. *Appl. Catal. B.* **2015**, *166*, 535–543. [[CrossRef](#)]
14. Badmaev, S.D.; Pechenkin, A.A.; Belyaev, V.D.; Sobyenin, V.A. Hydrogen production by steam reforming of dimethoxymethane over bifunctional CuO-ZnO/γ-Al<sub>2</sub>O<sub>3</sub> catalyst. *Int. J. Hydrogen Energy* **2015**, *40*, 14052–14057. [[CrossRef](#)]
15. Joó, F. Breakthroughs in Hydrogen Storage-Formic Acid as a Sustainable Storage Material for Hydrogen. *ChemSusChem* **2008**, *1*, 805–808. [[CrossRef](#)] [[PubMed](#)]
16. Bulushev, D.A.; Beloshapkin, S.; Ross, J.R.H. Hydrogen from formic acid decomposition over Pd and Au catalysts. *Catal. Today* **2010**, *154*, 7–12. [[CrossRef](#)]
17. Zhou, X.; Huang, Y.; Xing, W.; Liu, C.; Liao, J.; Lu, T. High-quality hydrogen from the catalyzed decomposition of formic acid by Pd-Au/C and Pd-Ag/C. *Chem. Commun.* **2008**, *30*, 3540–3542. [[CrossRef](#)]
18. Tedsree, K.; Li, T.; Jones, S.; Chan, C.W.A.; Yu, K.M.K.; Bagot, P.A.J.; Marquis, E.A.; Smith, G.D.W.; Tsang, S.C.E. Hydrogen production from formic acid decomposition at room temperature using a Ag-Pd core-shell nanocatalyst. *Nat. Nanotechnol.* **2011**, *6*, 302–307. [[CrossRef](#)]

19. Fellay, C.; Dyson, P.; Laurency, G. A Viable Hydrogen-Storage System Based On Selective Formic Acid Decomposition with a Ruthenium Catalyst. *Angew. Chem. Int. Ed.* **2008**, *47*, 3966–3968. [[CrossRef](#)]
20. Bulushev, D.A.; Chuvilin, A.L.; Sobolev, V.I.; Stolyarova, S.G.; Shubin, Y.V.; Asanov, I.P.; Ishchenko, A.V.; Magnani, G.; Riccò, M.; Okotrub, A.V.; et al. Copper on carbon materials: Stabilization by nitrogen doping. *J. Mater. Chem. A* **2017**, *5*, 10574–10583. [[CrossRef](#)]
21. Gazsi, A.; Bánsági, T.; Solymosi, F. Decomposition and Reforming of Formic Acid on Supported Au Catalysts: Production of CO-Free H<sub>2</sub>. *J. Phys. Chem. C* **2011**, *115*, 15459–15466. [[CrossRef](#)]
22. Solymosi, F.; Koós, Á.; Liliom, N.; Ugrai, I. Production of CO-free H<sub>2</sub> from formic acid. A comparative study of the catalytic behavior of Pt metals on a carbon support. *J. Catal.* **2011**, *279*, 213–219. [[CrossRef](#)]
23. Iglesia, E.; Boudart, M. Decomposition of formic acid on copper, nickel, and copper-nickel alloys: II. Catalytic and temperature-programmed decomposition of formic acid on Cu/SiO<sub>2</sub>, Cu/Al<sub>2</sub>O<sub>3</sub>, and Cu powder. *J. Catal.* **1983**, *81*, 214–223. [[CrossRef](#)]
24. Caputo, T.; Lisi, L.; Pirone, R.; Russo, G. On the role of redox properties of CuO/CeO<sub>2</sub> catalysts in the preferential oxidation of CO in H<sub>2</sub>-rich gases. *Appl. Catal. A. Gen.* **2008**, *348*, 42–53. [[CrossRef](#)]
25. Jiang, X.Y.; Lou, L.P.; Chen, Y.X.; Zheng, X.M. Effects of CuO/CeO<sub>2</sub> and CuO/γ-Al<sub>2</sub>O<sub>3</sub> catalysts on NO + CO reaction. *J. Mol. Catal. A. Chem.* **2003**, *197*, 193–205.
26. Menon, U.; Poelman, H.; Bliznuk, V.; Galvita, V.V.; Poelman, D.; Marin, G.B. Nature of the active sites for the total oxidation of toluene by CuO-CeO<sub>2</sub>/Al<sub>2</sub>O<sub>3</sub>. *J. Catal.* **2012**, *295*, 91–103. [[CrossRef](#)]



© 2019 by the authors. Licensee MDPI, Basel, Switzerland. This article is an open access article distributed under the terms and conditions of the Creative Commons Attribution (CC BY) license (<http://creativecommons.org/licenses/by/4.0/>).